J MATER SCI **41** (2006) 1213–1219

Dispersion and rheology of nickel nanoparticle inks

WENJEA J. TSENG*, CHUN-NAN CHEN
Department of Materials Engineering, National Chung-Hsing University, 250 Kuo Kuang Road, Taichung, 402, Taiwan
E-mail: wenjea@dragon.nchu.edu.tw

Published online: 4 February 2006

Nickel nanoparticles were dispersed in α-terpineol solvents, and their rheological behaviour and suspension structure were examined using various organic surfactants, surfactant concentrations (0–10 wt.% of the powder) and solids loadings (ϕ=0.01–0.28 in volumetric ratios) over a shear-rate range 10^0–10^3 s^{-1}. A surfactant of oligomer polyester was found effective in the nanoparticle dispersion. An optimal surfactant concentration ca. 2–4 wt.% of the solids was found; beyond which, the apparent viscosity increased adversely. The oligomer-polyester molecules appeared to adsorb preferentially on the nanoparticle surface, forming a steric layer which facilitates the ink flow for the improved dispersion. A pseudoplastic flow behaviour was found as shear rate increased, and a maximum solids concentration (ϕ_m) was estimated as ϕ_m=0.32. The interparticle potential was dominated by van der Waals attraction in the terpineol liquid, and a reaction-limited cluster aggregation (RLCA) featuring with a fractal dimension (D_f) of 2.0 was calculated. This finding together with the reduced ϕ_m reveals that the nanoparticle inks were flocculated in character even with the presence of polyester surfactant. Additionally, a porous (electrically conductive) particulate network was expected to form if the inks were printed on a non-conductive substrate followed then by drying and sintering in practice.

1. Introduction

The increasing use of nickel (Ni) powders as a base-metal electrode (BME) in microelectronic devices has driven the development of nickel inks that can be printed or coated on dielectric substrates to form conductive thick films for multilayer electrical contacts and interconnections [1–5]. Thick-film process such as screen printing and direct writing often involves preparation of powdered inks (also called pastes) as a starting material [6–8]. In view of the literature, much effort has been devoted to the preparation of *micrometre-sized* nickel dispersions [9–13]. For example, Dutronc *et al*. [5] have investigated transport and detection properties when various metallic inks, including Ni pastes, were used as a thick-film electrode in semiconductor gas sensors. Antolini *et al*. [9] use glycerol trioleate as a dispersant to prepare Ni-ethanol mixtures for tape casting. Sánchez-Herencia *et al*. [10] have employed an ammonium salt of polyacrylic acid for stabilization of micrometre Ni powders in pure water. A maximum solids concentration up to 27 vol.% was obtained when an optimum concentration of polyacrylic surfactant was added in the aqueous colloids. Nadkarni *et al*. [11] have examined rheology of different metal pastes (including Ni alloys) for brazing and soldering applications. In our previous works, surfactant chemistry and its concentration were shown to be critically important to the dispersion and rheology of submicrometre Ni powders in α-terpineol [12] and ethanol-isopropanol [13] solvents. A dispersant of propylene glycol was found effective in providing a steric hindrance necessary for the stabilization of Ni dispersions.

With continuing refinement and advancement in multilayering and fine-line patterning of microelectronics, use of ultrafine powders in the ink formulation has becoming a technological trend in order to meet emerging requirements for further miniaturization of microelectronics and for higher frequency and reliability performance. To the author's knowledge, reports that address the preparation and dispersion of nickel nanoparticle inks aiming specifically for the hybrid thick-film processes are limited [14], despite the clear importance from technological viewpoints.

*Author to whom all correspondence should be addressed.
0022-2461
DOI: 10.1007/s10853-005-3659-z

One might suspect that the surface characteristics and the increased specific surface area involved in the nanoparticles would directly contribute to the difficulties in attaining stable nanoparticle dispersions, when compared to the micrometre-sized counterparts. In this regard, we intend to examine the dispersion and the resultant ink rheology and suspension structure when nanometre-sized Ni particles with a mean particle size <100 nm were dispersed in α-terpineol liquids. The terpineol solvent was chosen in the study as the liquid carrier because of its low vapor pressure at ambient temperature and its chemical compatibility with organic binders (e.g., ethylcellulose) frequently used in thick-film processes for manufacturing hybrid components [15, 16]. Various surfactants of polymeric nature were used and their dispersion qualities were examined by rheological characterizations. The polymeric surfactant molecules were thought to preferentially adsorb on the particle surface via their polar end, while the tail end of the molecules stretch toward the liquid medium for providing interparticle repulsions via the steric (or electrosteric) stabilization [17]. Flow property of the inks was hence altered by the surfactants addition to various extents, and the resultant ink structure was correlated to fractal geometry of aggregated clusters and compared with existing models in the study.

2. Experimental procedure

2.1. Materials

Nickel nanoparticles (Argonide Inc., U.S.A.) with an average particle size of about 90 nm, a specific surface area 4.5–7.5 m^2/g, and purity >99% were used as the starting material. The powder is about spherical in shape, as shown representatively in Fig. 1 from the transmission electron microscopy (TEM, JEM 2000FX, JEOL, Japan). An X-ray diffractometry (MAC Science, M18X-1180, Japan) with a Cu K_α radiation showed only diffraction peaks of pure, crystalline Ni phase. A field-emission scanning electron microscope (FE-SEM, JSM-6700F, JEOL, Japan) equipped with an energy-dispersive spectrometer yet revealed an existence of Cr, Si and some oxygen as minor impurities in the as-received Ni nanoparticles [18].

Seven commercially available organic surfactants were mixed with reagent-grade α-terpineol (90%, Aldrich Chemical Co., U.S.A.) independently before addition of the nanoparticles to form powdered inks with volumetric solids concentrations ϕ=0.01–0.28. The dispersants were polymeric polyelectrolytes with functional groups of cationic, anionic or nonionic feature. Their major compositions were indicated in Table I, consisting of amine, polyester and polyglycol as their major compositions. Surfactant concentration varied from 0.5 to 10% of the solids weight. Note that our objectives were to examine the fundamental dispersion and the resultant ink structure when the nanometre-sized Ni particles of different proportions were mixed with liquid terpineol; therefore, organic additives other than the surfactant molecules, such as plasticizers and binders often used in commercial inks, were neither added in the ink formulation nor of their effect on the ink rheology/structure considered in this study.

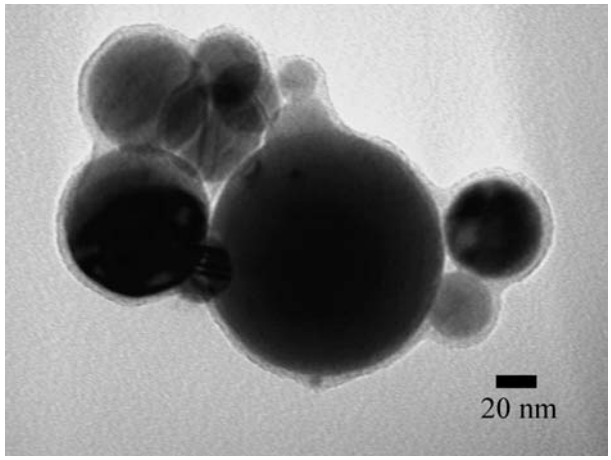

Figure 1 Morphology of Ni nanoparticles.

2.2. Rheological measurements

All the powdered inks were ball-mixed in polyethylene bottles using high-purity alumina balls as the mixing medium for a period of 24 h before their viscosity (η_s) was measured by a strain-controlled concentric viscometer (VT550, Gebruder HAAKE Gmbh, Germany) equipped with a sensor system (MV-DIN 53019, HAAKE, Germany) of a cone-cup geometry. All the rheological

TABLE I Polymeric surfactants used in the Ni nanoparticle — terpineol inks[a]

Designation	Major composition	Polarity	Specifications
KD-1	Polyester/Polyamine polymer	Weakly cationic	Powder form, acid number 19–31 mgKOH/g, base equivalent 1100–1600
KD-2	Polyoxyalkylene amine	Weakly cationic	Liquid form, base equivalent 1500–1950
KD-4	Oligomer polyester (polycondensed fatty acid)	Weakly anionic	Liquid form, acidic number 28–37 mgKOH/g
KD-5	Oligomer polyester	Weakly anionic	Pasty form, acidic number 66–77 mgKOH/g
KD-6	Propylene glycol	Non-ionic	Liquid form, acid value 6.0–12.0 mgKOH/g, HLB number 11–12
KD-7	Propylene glycol	Non-ionic	Liquid form, acid value 5 mgKOH/g
PS-2	Polyoxyalkylene amine derivative	Weakly cationic	Liquid form, base equivalent 1500–1950

[a]All the surfactants used are supplied by ICI Americas Inc., U.S.A.

measurements were conducted at a constant temperature (25°C). The measurement was performed with a steady increment of shear rate ($\dot{\gamma}$); to which, the rate was increased in every 1 s^{-1} over the shear-rate range of 1–10^1 s^{-1}, every 10^1 s^{-1} over 10^1–10^2 s^{-1} and every 10^2 s^{-1} over 10^2–10^3 s^{-1}. The rheological properties were all measured after 20 s of duration when the shear rate reached each pre-determined rate level over the entire shear-rate range examined. The ink dispersions typically reached an equilibrium stress at given shear rate in less than 10 s and kept at the stress level steadily over the remaining hold time in the measurement. The duration was then kept consistently throughout the measurement for all the inks prepared. Two samples were prepared and their viscosity measured for each ink formulation.

2.3. Structure, adsorption and interface

Some powdered inks were slip-casted onto plaster molds, and the dried cakes were examined by FE-SEM. The nanoparticles remained about spherical in shape, indicating that the impact force involved in the ball-mixing process did not deform the nanoparticles into "flake" forms considerably that might hinder the flow property and the resultant particle-packing structure of the ink dispersions. Some of the nanoparticle inks prepared were centrifuged at a rotational speed of 16,000 rpm and ultrasonically washed in fresh terpineol. The processes were repeated for four times before the centrifuged cakes were oven-dried at ~60°C for 48 h to remove the terpineol liquid. Thermogravimetric analysis (Netzsch Model 309A) with a precision of 0.01 mg was conducted on the dried granules with a heating rate of 10°C min^{-1} and up to 600°C in air. The weight loss thus determined is the amount of surfactant molecules that adhere strongly on the particle surface in the terpineol liquid under the severe shearing environment. Contrarily, the molecules that were separated from the powders after the repeated centrifugation and washing processes were considered either loosely adsorbed or even free (depleted) molecules existing in the liquid solvent. An adsorption isotherm of the surfactant molecules to the Ni nanoparticle surface was then determined.

3. Results and discussion

3.1. Surfactant screening

Apparent viscosities of the Ni nanoparticle—terpineol mixtures are listed in Table II when various polymeric surfactants were used in the ink formulation respectively. Solids concentration of the inks was held constant at ϕ=0.1, so as the surfactant concentration at 2 wt.% of the solids. The ink viscosity reduces to various extents upon the surfactants addition, and the reduction appears to depend critically on the surfactant chemistry and the applied shear rate. Among the polymeric surfactants examined, oligomer polyesters with a weakly anionic feature (i.e., KD-4 and KD-5) appear to be the most effective. The viscosity reduction is particularly pronounced for the inks with the KD-4 surfactant; to which, a reduction as much as 40–70% was seen found at the shear-rate regime often encountered in most screen-printing and tape-casting processes ($\dot{\gamma}$ = 10–100 s^{-1}) [19]. In addition, the viscosity of the KD-4 inks in absolute values also reduces as shear rate increased. This reveals that the nanoparticle inks were in fact *flocculated* in character despite the presence of oligomer polyester; therefore, Ni aggregates were remained in the liquid carrier after the prolonged ball mixing (24 h), even though the aggregates decreased in size when compared to that of the aggregates prior the mixing process. This led to the reduced overall flow resistance and hence a decreased apparent viscosity.

TABLE II Apparent viscosities of the Ni nanoparticle inks (ϕ=0.1) at shear rates of 10, 100 and 1000 s^{-1} when different polymeric surfactants were used in the ink formulation. The dispersant concentration was held constant at 2 wt.% of the solids

	η_s (mPa·s)		
Dispersant type	$\dot{\gamma}$ = 10 s^{-1}	$\dot{\gamma}$ = 100 s^{-1}	$\dot{\gamma}$ = 1000 s^{-1}
No Dispersant	606.1 (100%)	154.5 (100%)	78.7 (100%)
KD-1	317.1 (52%)	122.6 (79%)	79.6 (101%)
KD-2	404.9 (67%)	122.0 (79%)	73.6 (94%)
KD-4	189.0 (31%)	92.6 (60%)	70.6 (90%)
KD-5	271.9 (45%)	100.0 (65%)	68.6 (87%)
KD-6	307.4 (51%)	99.5 (64%)	64.6 (82%)
KD-7	402.8 (67%)	115.3 (75%)	63.6 (81%)
PS-2	593.8 (98%)	143.5 (93%)	73.7 (94%)

The numbers in parentheses are the ratios of viscosities at specific shear rates.

Figure 2 shows the dependence of ink viscosity with oligomer concentration. An optimal concentration occurs alongside with a reduced viscosity at about 2–4 wt.% of the solids. The ink viscosity then increases adversely as the surfactant concentration is increased, reaching a viscosity level comparable to that of the inks without any surfactant. The ink viscosity further rises upon an additional surfactant fraction above 10 wt.%, judged from

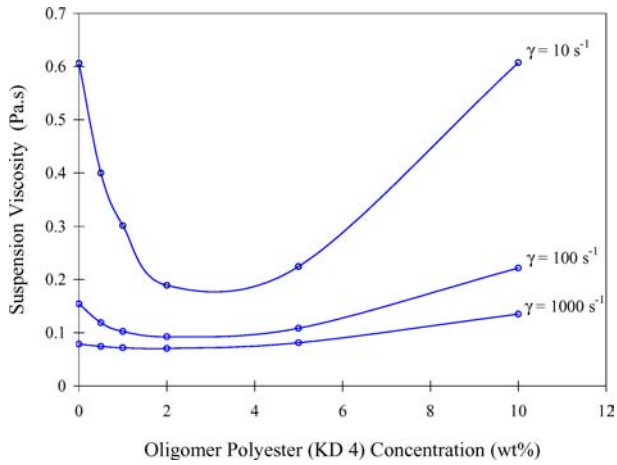

Figure 2 The dependence of ink viscosity to the concentration of oligomer polyester (KD-4) surfactants.

visual inspections because of the apparent viscosity of the inks well exceeded the upper bound of the detection limit of the viscometer rotor employed.

In Fig. 3, an adsorption isotherm of the oligomer polyester (KD 4) on the Ni nanoparticle surfaces indicates a Langmuir-type adsorption behaviour in the terpineol liquid. The specific adsorption quickly rises to a level as the oligomeric polyester was slightly introduced into the terpineol liquid. The adsorption then gradually reaches a saturation plateau (~4 mg/m^2) as the oligomer concentration increases above ~2 wt.% (corresponding to exactly 2 mg of the oligomer polyester per milli-liter of the terpineol liquid). This finding is in good agreement with the optimal surfactant concentration found in the viscosity measurement (Fig. 2), and suggests that the preferentially adsorbed polymeric molecules on the nanoparticle surface provide an effective steric (and/or electro-steric) layer which keeps the nanoparticles (or clusters) apart from re-aggregation into a continuous particle network possessing a stronger resilience to shear deformations.

It may be interesting to note that the most effective surfactant for the nickel powders of *micrometre* size in terpineol solvent was the non-ionic polymeric dispersant, i.e., KD-6 and KD-7, in our earlier report [12]. This finding is different from what we have observed for the nanoparticle counterpart. In spite of the difficulty in knowing the real composition and molecular structure of the commercial dispersants, we suspect that the surface chemistry of the nickel nanoparticles plays a critical role in determining the dispersion efficacy. The chemical aspect of particle surfaces may differ substantially, and this difference would affect the driving force for the surfactant molecules to adsorb preferentially at the solid-solvent interface to lower the interfacial free energy [20]. This in turn affects the active sites available on the particle surface allowable for anchoring with the active groups of the surfactant molecules. Population density of the molecular active groups is vital in determining the adsorption affinity of polymeric surfactants to the nickel particles. The denser the surfactant packing at the interface, the larger the reduction in surface tension is anticipated, which in turn is beneficial for the suspension flow.

3.2. Rheology of Ni nanoparticle inks

The concentrated nanoparticle inks generally exhibit a shear-thinning flow character over the solids-loading and shear-rate regimes examined. As shown in Fig. 4, the viscosities of inks reduce linearly as shear rate is increased in a logarithmic plot when solids concentration exceeds 0.05 at the lower shear-rates range ($\dot{\gamma} < \sim 100\ s^{-1}$). The shear-thinning flow is in parallel with the findings of Table II in a sense that the formation of powdered aggregates was energetically favorable in the concentrated inks with the oligomer polyester. Van der Waals attraction is involved in the nanoparticle aggregation [19], and a spatially definable ink structure may be formed in the liquid [21–23]. A further increase in the applied shear force appears to break down the ink network to a certain extent so that the resistance to flow is reduced, particularly at the low shear-rate regime. The inks apparently become more of a Bingham-typed flow or even a slightly dilatant (i.e., shear thickening) flow when shear rate is further increased toward the higher ends (Fig. 4). The Bingham and shear-thickening flow behaviours become apparently more pronounced for the inks with a reduced solids concentration ($\phi < 0.05$).

Barnes [24] has indicated that powdered suspensions in a shear-thinning regime tend to become a two-dimensional, layered arrangement as shear rate increases toward infinity. This would result in a structural evolution in the ink as a function of shear rate. A rather dense particle-packing structure is favorable to form in compliance with the increasing shear forces, and hence a less sensitive suspension structure is attained with the shear-rate increase, leading to a Bingham-typed flow character. The suspension structure may then be abruptly changed toward a three-dimensional, more random type of particulate arrangement involving a larger filling space of flow movement as shear rate exceeds a critical level. This

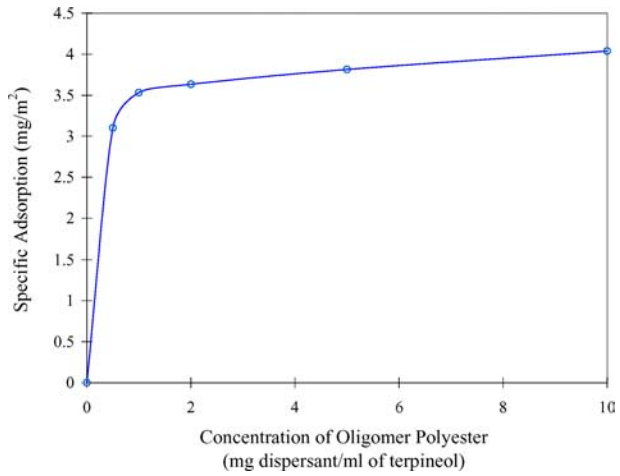

Figure 3 The adsorption isotherm of oligomer polyester (KD-4) on Ni nanoparticle surface in the terpineol liquid.

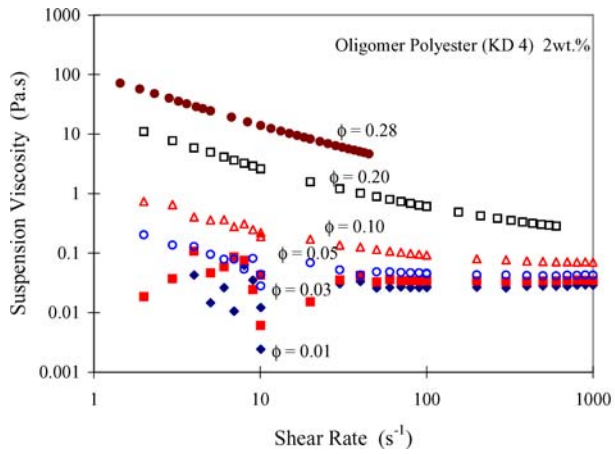

Figure 4 Ink viscosity as a function of the applied shear rate in a logarithmic plot. The solids concentration varies from ϕ=0.1 to ϕ=0.28.

structural change is accompanied with an increase in viscosity, because the fluid dilation occurs when the ink flow changes toward a more turbulent type of flow from an "original" lamellar flow. Cause of the dilatancy is not clear at present, and includes possible mechanisms such as local inhomogeneities existing in the ink structure, e.g., particle-size distribution, difference in particle shape, surface "roughness", etc. The viscosity "scattering" found in the inks (Fig. 4) with reduced solids concentrations (ϕ<0.05) is mainly due to the viscosity measured at the lower shear-rate range fell in a range of the lower bound of the detecting sensor employed, and is merely good for reference purposes.

3.3. ϕ_m Determination of Ni nanoparticle inks

Relative viscosity (η_r) of the inks may be defined as the ink viscosity dividing by the viscosity of the carrier fluid, and is plotted against the solids concentration (ϕ) at a given shear rate of 100 s^{-1} in Fig. 5. The η_r increases notably as ϕ exceeds a critical concentration, $\phi_c \sim 0.15$. An exponential form of $\eta_r = 0.86 \exp(19.4\,\phi)$ appears to fit the experimentally determined $\eta_r - \phi$ relationship reasonably well over the broad solids-concentration range examined. The physical meaning of the exponential form may not be of substantial significance; yet, the relatively large exponent value, i.e., 19.4, reveals a strong dependence of η_r to ϕ when the nanoparticle inks become literally "crowded" in the suspensions. This finding hence serves as an experimental evidence reiterating the importance of interparticle reaction forces in the determination of macroscopic flow behaviour of the nanoparticle mixtures. This conclusion is justifiable in flocculated suspension systems of various chemistries and particle sizes [25].

The solids concentration of the Ni inks is thought critically important to ensure an electrically conductive path in the microelectronic thick-film devices, and a higher solids concentration is often desirable from this perspective. A recent model proposed by Liu [26] is used in the study to

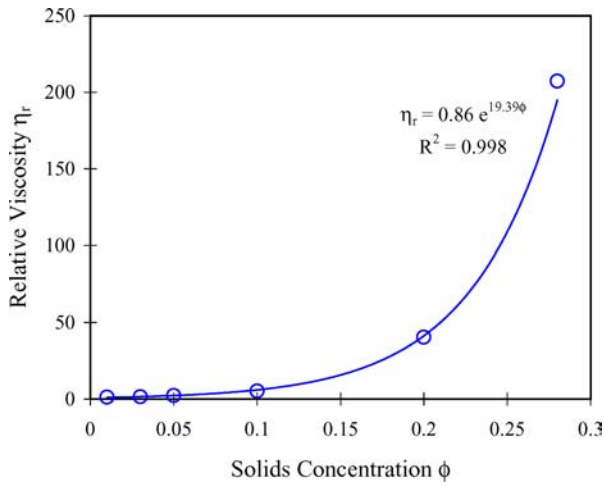

Figure 5 Relative viscosity (η_r) of the inks as a function of solids concentration (ϕ).

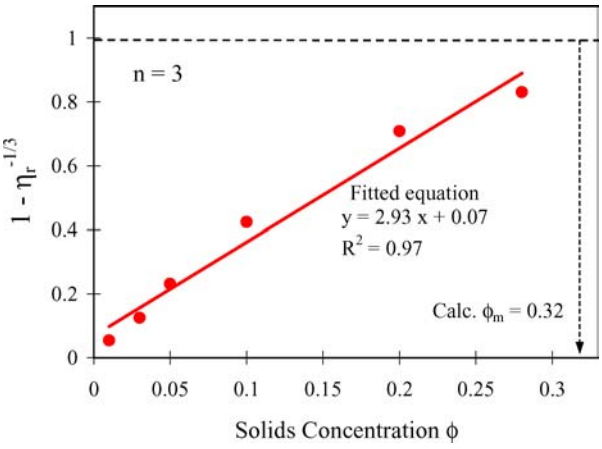

Figure 6 A derivative of η_r, i.e., $1 - \eta_r^{-1/3}$, as a function of solids concentration (ϕ).

estimate the maximum solids concentration (ϕ_m) attainable for the Ni nanoparticle inks examined. The model originates from an observation that

$$1 - \eta_r^{-1/n} = f(\phi) \tag{1}$$

where n is a structure-dependent parameter. The exponent n has a value between n=2 to 3 for several suspension systems involving powders of various chemistries, particle-size distributions and organic vehicles over a broad shear-rate range [12, 13, 26]. Fig. 6 shows the $(1-\eta_r^{-1/3}) - \phi$ dependence of the inks. An approximately linear relationship is resulted with a satisfactory correlation factor (R^2=0.97), and ϕ_m may hence be determined from the fitted equation by extrapolating the linear line to $1 - \eta_r^{-1/3} \rightarrow 1$ at which $\eta_r \rightarrow \infty$. This operation gives ϕ_m=0.32 for the Ni inks, and the calculated ϕ_m compares favorably with the $\eta_r - \phi$ dependence shown in Fig. 5; to which, the viscosity approaches infinity at solids concentration ϕ exceeds ~0.3. This calculated ϕ_m is substantially lower than that of the random close packing ($\phi_m \sim 0.64$) of monosized spheres, and it further vindicates the existence of nanoparticle aggregations in the carrier liquid.

The Ni nanoparticles were also dispersed in pure water and the ϕ_m determined was ϕ_m=0.28 at an identical shear rate of 100 s^{-1} [14]. The calculated ϕ_m in pure water is not very different from that of the aforementioned Ni-terpineol system (ϕ_m=0.32). Therefore, use of water instead of terpineol solvent is also a viable route to fabricate Ni-BME components in practice and is more environmentally friendly from ecological viewpoint. Yet, the selection of binder/plasticizer is somehow limited when water is used as the dispersing solvent.

3.4. Yield stress and particulate structure of Ni nanoparticle inks

Maintaining a high dispersion quality at all stages of screen-printing and tape-casting processes is of critical

importance for attaining a defect-free, sintered thick-film structure. An ink of low viscosity is generally desirable at relatively high shear rate for the ease of forming; whilst, a concentrated ink of high solids loading provides a suitable yield stress for maintaining the shape after removal of the forming stress, and a desired electrical properties after sintering as well. The yield stress (τ_y) of the nanoparticle inks can be estimated from the Casson equation [19]:

$$\tau^{1/2} = \tau_y^{1/2} + (\eta_s \cdot \dot{\gamma})^{1/2} \quad (2)$$

Fig. 7 shows the linear $\tau^{1/2} - \dot{\gamma}^{1/2}$ dependence over the solids concentrations investigated. By extrapolating the curve-fitted, linear lines to $\dot{\gamma} \rightarrow 0$, τ_y of the inks is determined. As shown in Fig. 8, τ_y appears to increase pronouncedly as ϕ exceeds ~0.15.

A quantitative evaluation of the ink structure can be obtained from the $\tau_y - \phi$ dependence using fractal geometry. Shih *et al.* [26] suggested that τ_y scales with ϕ in the following form for flocculated suspension systems:

$$\tau_y \sim (1 - 1.5\alpha\zeta^2)(A/24s_o^{3/2})(1/R^{d-3/2})\phi^m \quad (3)$$

where α is a constant related to the Debye thickness (κ^{-1}) and the surface separation (s_o) between particles; ζ the zeta potential; A the Hamaker constant; R the particle radius; d the Euclidean dimension; and $m = (d + X)/(d - D_f)$ with D_f and X the fractal dimension of the clusters and the backbone of the clusters, respectively. The backbone of the cluster (X) may be assumed as X=1 [26]. Considering the fractal geometry in three dimensions, the Euclidean dimension (d) has a value d=3. D_f is hence correlated with the rheological properties and can be determined once m becomes available.

From the power-law fit shown in Fig. 8, m was determined as m=4.22 (R^2=0.995). The calculated D_f is then D_f=2.0 for the nanoparticle inks consisting of 2 wt.% oligomer polyester (KD-4) as a dispersant. The calculated D_f matches exactly with that of the reaction-limited cluster-cluster aggregation (RCLA, D_f=2 from measurement of various scattering techniques [19]). This reveals that particle rearrangement is possible to occur in the aggregated structure. Since the addition of oligomer polyester did not provide a full stabilization for the nanoparticle inks and the inks was still flocculated structurally. This freedom of relative particle movement stems presumably from the adsorbed surfactant molecules on the nanoparticle surface, which reduce the interparticle attraction by physically increasing the interparticle spacings in the carrier liquid. A denser particle-packing structure would be resulted when compared to that of the suspension structure involving purely attractive forces between particles.

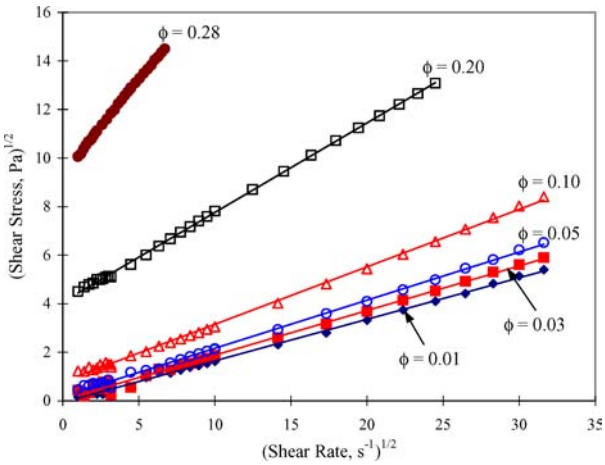

Figure 7 The (shear stress)$^{1/2}$ vs. (shear rate)$^{1/2}$ relationship for determining the yield stresses of the inks.

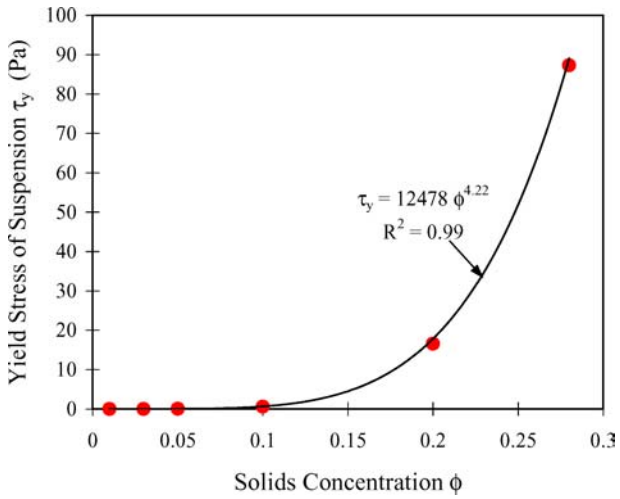

Figure 8 Yield stresses of the nanoparticle ink as a function of solids concentration (ϕ).

4. Conclusion

A polymeric surfactant consisting of oligomer polyester as its major composition reduced the flow resistance of Ni nanoparticle—terpineol inks with an improved dispersion quality. Maximum viscosity reduction as much as 40–70% was found at shear-rate regimes often encountered in most screen-printing and tape-casting processes ($\dot{\gamma}$ = 10–100 s^{-1}). The surfactant molecules appeared to preferentially adsorb on the nanoparticle surface via a Langmuir-typed adsorption. This organic adsorption layer is thought to provide a steric hindrance which inhibits the nanoparticles (or clusters) in the terpineol liquid from re-aggregating into a connected particulate network that presents a stronger resistance to flow deformation. The nanoparticle inks generally showed a shear-thinning flow behaviour as shear rate increased, suggesting a continuing breakdown of the flow clusters into smaller flow units. The inks then changed toward a Bingham-typed or shear-thickening flow behaviour as the shear rate further increased. Despite the surfactant addition, the nanoparticle inks were still flocculated in character. A fractal calculation revealed that the interparticle attraction might have

reduced to a certain extent so that particle re-arrangement is allowed to occur.

Acknowledgments

The surfactant samples were provided by Mr. Tony Y. C. Lee of the Green Chem Taiwan Co., Ltd. The authors gratefully acknowledge the National Science Council (Taiwan, R.O.C.) for funding this research under contracts NSC 90-2216-E-034-010 and 91-2216-E-005-024. This work was partly conducted at the Institute of Materials Science and Manufacturing, Chinese Culture University (Taiwan).

References

1. M. VOLLMANN, R. HAGENBACK and R. WASER, *J. Am. Ceram. Soc.* **80**(9) (1997) 2301.
2. S. SUMITA, M. IKEDA, Y. NAKANO, K. NISHIYAMA and T. NOMURA, *ibid.* **74**(11) (1991) 2739.
3. H. SHOJI, Y. NAKANO, H. MATSUSHITA, A. ONOE, H. KANAI and Y. YAMASHITA, *J. Mater. Synth. Process* **6**(6) (1998) 415.
4. D. J. MALANGA and B. T. BASSLER, *Am. Ceram. Soc. Bulletin* **79**(9) (2000) 49.
5. P. DUTRONC, B. CARBONNE, F. MENIL and C. LUCAT, *Sensors and Actuators B* **6** (1992) 279.
6. J. E. SMAY, J. CESARANO III and J. A. LEWIS, *Langmuir* **18** (2002) 5429.
7. D. B. CHRISEY, *Science* **289** (2000) 879.
8. J. J. LICARI, in *Electronic Materials & Processes Handbook* (McGraw-Hill, Inc., New York, 1993) p. 8.1.
9. E. ANTOLINI, M. FERRETTI and S. GEMME, *J. Mater. Sci.* **31** (1996) 2187.
10. A. J. SÁNCHEZ-HERENCIA, A. J. MILLÁN, M. I. NIETO and R. MORENO, *Acta Mater.* **49** (2001) 645.
11. A. V. NADKARNI, G. L. COWAN, A. V. CARRARD and R. KHATTAR, *Int. J. Powder Metall.* **37** (2001) 49.
12. W. J. TSENG and C.-N. CHEN, *Mater. Sci. Eng. A* **347**(1–2) (2003) 145.
13. W. J. TSENG and S.-Y. LIN, *ibid.* **362**(1–2) (2003) 165.
14. W. J. TSENG and C.-N. CHEN, *J. Mater. Sci. Lett.* **21**(5) (2002) 419.
15. E. S. THIELE and N. SETTER, *J. Am. Ceram. Soc.* **83**(6) (2000) 1407.
16. C.-J. HSU and J.-H. JEAN, *Mater. Chem. Phys.* **78** (2002) 323.
17. K. HOLMBERG, B. JÖNSSON, B. KRONBERG and B. LINDMAN, *Surfactants and Polymers in Aqueous Solution* (John Wiley & Sons, Ltd., Hoboken, New Jersey, U.S.A., 2003) p.
18. W. J. TSENG, C. K. HSU, C.-C. CHI and K.-H. TENG, *Mater. Lett.* **52**(4–5) (2002) 313.
19. R. J. PUGH and L. BERGSTRÖM, *Surface and Colloid Chemistry in Advanced Ceramics Processing* (Marcel Dekker, Inc., New York, U.S.A., 1994) p. 279.
20. K. HOLMBERG, B. JÖNSSON, B. KRONBERG and B. LINDMAN, *Surfactants and Polymers in Aqueous Solution* (John Wiley & Sons, Ltd., New Jersey, U.S.A., 2003) p. 357.
21. W.-H. SHIH, W. Y. SHIH, S.-I. KIM, J. LIU and I. A. AKSAY, *Phys. Rev. A: Gen. Phys.* **42** (1990) 4772.
22. C. ALLAIN, M. CLOITRE and M. WAFRA, *Phys. Rev. Lett.* **74**(8) (1995) 1478.
23. J. C. SÁNCHEZ-LÓPEZ and A. FERNÁNDEZ, *Acta Mater.* **48** (2000) 3761.
24. H. A. BARNES, *J. Rheol.* **33** (1989) 329.
25. C.-N. CHEN and W. J. TSENG, *J. Mater. Sci.* **39** (2004) 3471.
26. D.-M. LIU, *ibid.* **35** (2000) 5503.
27. W. Y. SHIH, W.-H. SHIH and I. A. AKSAY, *J. Am. Ceram. Soc.* **82**(3) (1999) 616.

Received 27 July 2004
and accepted 25 May 2005